Papers presented at the Workshop on
Short Pulse High Current Cathodes
Bendor, France, June 18-22, 1990

BNL–45469

PHOTOEMISSION STUDIES USING FEMTOSECOND PULSES FOR HIGH BRIGHTNESS ELECTRON BEAMS*

T. Srinivasan-Rao, T. Tsang, and J. Fischer

Brookhaven National Laboratory, Upton, NY 11973

June 1990

BNL--45469

DE91 008436

PHOTOEMISSION STUDIES USING FEMTOSECOND PULSES FOR HIGH BRIGHTNESS ELECTRON BEAMS*

T. Srinivasan-Rao, T. Tsang and J. Fischer
Brookhaven National Laboratory
Upton, NY 11973

ABSTRACT

We present the results of a series of experiments where various metal photocathodes are irradiated with ultrashort laser pulses, whose characteristics are: λ = 625 nm, τ = 100 fs, PRR = 89.5 MHz, $h\nu$ = 2 eV and average power 25 mW in each of the two beams. The quantum efficiency of the metals range from $\sim 10^{-12}$ to 10^{-8} at a power density of 100 MW/cm^2 at normal incidence. Since all the electrons are emitted due to multiphoton processes, these efficiencies are expected to increase substantially at larger intensities. The efficiency at 100 MW/cm^2 has been increased by using *p*-polarized light at oblique incidence by $\sim 20\times$ and by mediating the electron emission through surface plasmon excitation by $\sim 10^3\times$. For the low intensities used in these experiments, the electron pulse duration is almost the same as the laser pulse duration for both the bulk and the surface plasmon mediated photoemission.

*This research was supported by the U.S. Department of Energy: Contract No. DE-AC02-76CH00016.

Recently, there has been increased interest in generating electron beams with very high brightness and low emittance for applications such as the laser LINAC,[1] short wavelength FEL,[2] and nonlinear Compton scattering.[3] The emittance of the electrons leaving the cathode increases as the square root of the kinetic energy of the electrons, dictated by their temperature and the excess energy of the photon over the work function. The kinetic energy, and hence the emittance may be reduced by operating the photocathode in a nonlinear photoemission regime.[4] In transport, the emittance of the electrons increases further due to space charge. For a given field and current density, this can be minimized by maintaining the electron bunch length small compared to the interelectrode gap.[5] This short electron bunch also reduces emittance due to RF dynamics in an RF cavity by reducing the change in the accelerating field experienced by the electrons in different longitudinal sections of the bunch as they leave the cathode. One scheme to generate such short bunches of electrons is irradiating the photocathode with subpicosecond laser pulses. Some of the applications mentioned above call for current densities exceeding 1 kA/cm^2. These requirements impose restrictions on the choice of the photocathode material.

The photocathode has to be efficient enough to yield these high current densities before the onset of optical damage to the cathode surface and yet maintain low kinetic energy of the electrons. Irradiation using a

laser of pulse duration shorter than the electron phonon relaxation time of the photocathode material may give rise to high electron temperature without significant heating of the lattice,[6] which could degrade the emittance and elongate the electron bunch. Hence, measurement of the quantum efficiency, the electron pulse duration, and temperature is very important in successful application of this scheme. In the subsequent sections, we present our results of these measurements along with different schemes to enhance the efficiency.

EFFICIENCY

The schematic of the experimental arrangement to measure the efficiency is shown in Fig. 1. The laser system used is an unamplified Colliding Pulse Mode locked (CPM) ring dye laser operating at a repetition rate of 89.5 MHz, pulse duration of ~100 fs at 625 nm and dual beam output, each with an average power of ~25 mW. One of the output beams is passed through a $\lambda/2$ plate and a polarizer, acting together as a variable attenuator for the laser power. A 5 cm focal length lens is used to focus the beam normally onto the target photocathode. The second beam is used for characterizing the laser beam. The photocathode preparation consists of the following steps: a disc machined from high purity metal is attached to a copper plug, polished with 1 μm diamond-based polishing compound, cleaned in an ultrasonic hexane bath, and dried with N_2. The diode is then

assembled, the electrode gap set in N_2 atmosphere, and installed in the vacuum chamber, where it is pumped down to 10^{-8}–10^{-9} Torr. Prior to efficiency measurements, the cathodes are activated by irradiating them *in situ* with a laser pulse of 10 ps duration, 266 nm wavelength and ~10 mJ/cm^2 energy density.

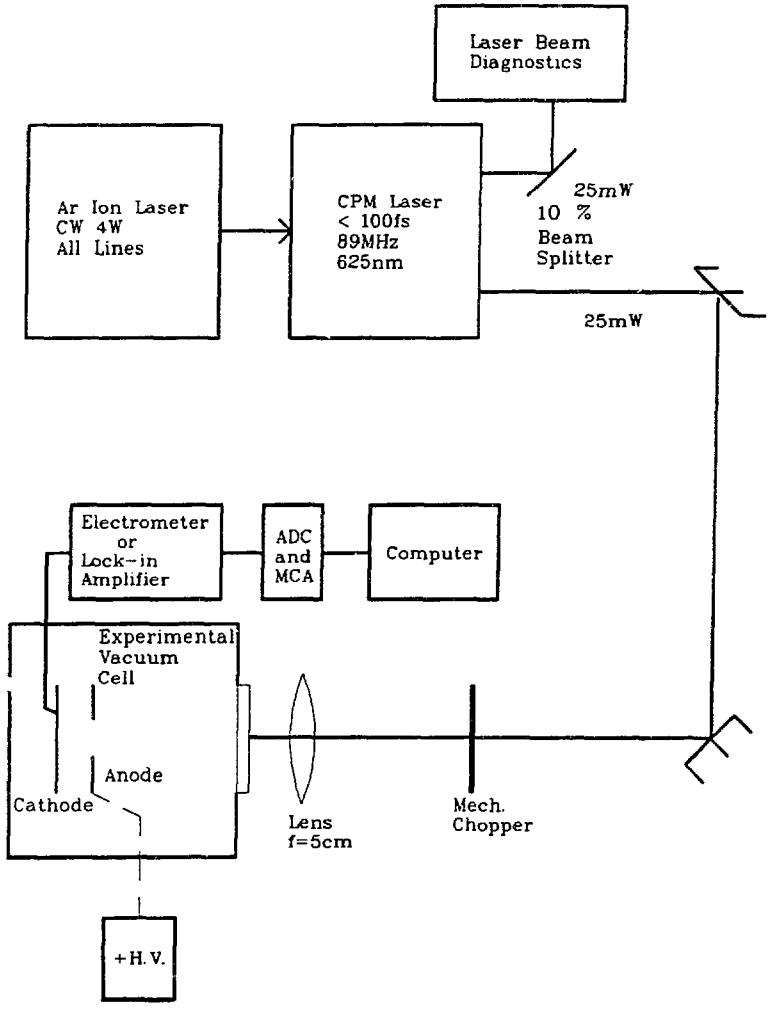

1) Schematic of the experimental arrangement to measure the quantum efficiency of the photoemission process.

The vacuum chamber consists of a fused silica window, an anode with an opening for the passage of the laser light and a cathode held parallel to the anode. The electrode gap, set prior to installation, can be varied from .3–1 mm. The anode is biased at +500 V and the average current leaving the cathode is fed to a picoammeter. The output current density measured as a function of input laser intensity for various metals is illustrated in Fig. 2. The efficiencies measured at 100 MW/cm^2 are listed in Table 1.

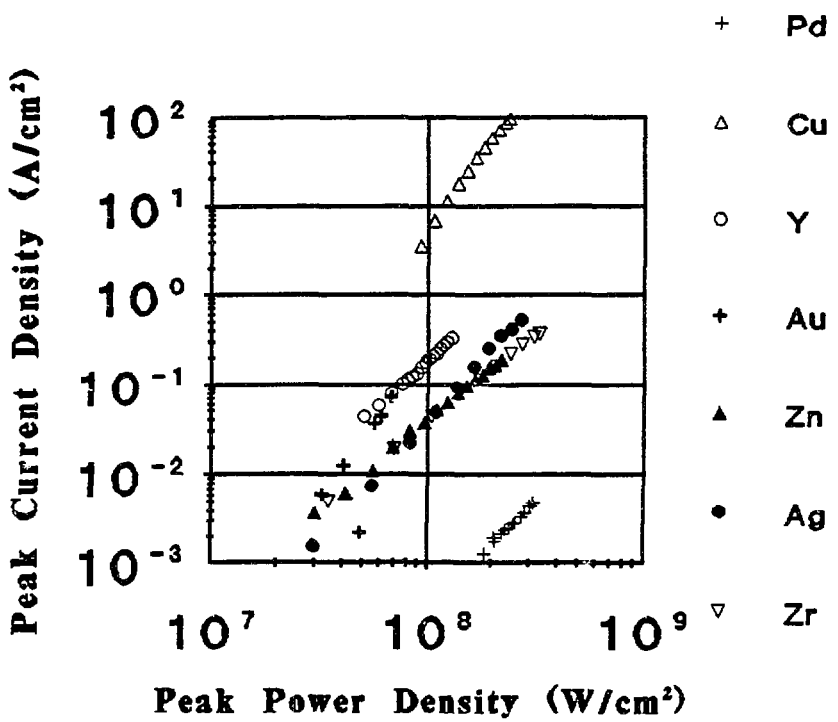

2) Electron emission from bulk metals, upon irradiation with a 625 nm, 100 fs laser pulse at normal incidence. The slope of the line is N, the number of photons required for the electron emission. The quantum efficiency of the process and N are listed in Table 1.

Table I

Laser Beam Characteristics

λ = 625 nm, τ = 100 fs PRR = 89.5 MHz

Material	Work Function[a]	Efficiency[b] at 100 MW/cm^2	Number of Photons Involved[c]
Yttrium	2.9[d]	4.0×10^{-9}	2.2
Zinc	3.7	8.0×10^{-10}	2.15
Gold	4.3	5.0×10^{-9}	3.25
Palladium	5.0	7.0×10^{-12}	2.5
Silver	4.3	1.0×10^{-9}	2.68
Nickel	4.4	$< 10^{-12}$	-----
Zirconium	4.3	8.0×10^{-10}	1.93
Platinum	5.3	4.0×10^{-12}	2.8
Copper	4.4	$\sim 10^{-9}$ [e]	3–3.57

[a] Data taken from literature, e.g., C.R.C. Handbook of Chemistry and Physics.

[b] Efficiency is defined as the number of electrons emitted per incident photon.

[c] Obtained from the slope of Fig. 2.

[d] Measured.

[e] Efficiency of copper is very sensitive to material and surface quality, and ranged from 8×10^{-8} to 1×10^{-10}.

ENHANCEMENT OF EFFICIENCY DUE TO POLARIZATION DEPENDENCE

Theory

When a linearly polarized light incidents on a smooth surface at an oblique angle, the absorption of light is a strong function of the angle of polarization. The transmittance[7] of *p*- and *s*-polarized light are,

$$T_p = \frac{2 \sin\theta_t \cos\theta_i}{\sin(\theta_i + \theta_t)\cos(\theta_i - \theta_t)} \quad A_p \tag{1}$$

$$T_s = \frac{2 \sin\theta_t \cos\theta_i}{\sin(\theta_i + \theta_t)} \quad A_s \tag{2}$$

$$T_p \geq T_s \tag{3}$$

Where θ_i = Angle of incidence.

θ_t = Angle of refraction, complex if the medium is a metal.

A_p = Amplitude of the electric field parallel to the plane of incidence.

A_s = Amplitude of the electric field normal to the plane of incidence.

The electron emission from a metal surface has two components, one arising from direct absorption of photon and the other due to the component of the laser induced electric field A_{p1} normal to the metal surface in the plane of incidence as shown in Fig. 3. If the total current density emitted is the algebraic sum of these two contributions, then;

$$j_p \propto \left(\sqrt{\alpha_p}\, T_p + A_{pI}\right)^{2N} \tag{4}$$

$$j_s \propto \left(\sqrt{\alpha_p}\, T_s\right)^{2N} \tag{5}$$

Where α_p and α_s are the absorption coefficients for p- and s-polarized light, respectively. The p-polarized light would yield larger current than the s-polarized light due to an increased absorption and the presence of the component of the electric field associated with the laser normal to the cathode surface. Measurement of $R_s = (1 - T_s)$, $R_p = (1 - T_p)$, j_s and j_p would enable us to calculate the enhancement due to the two effects individually.

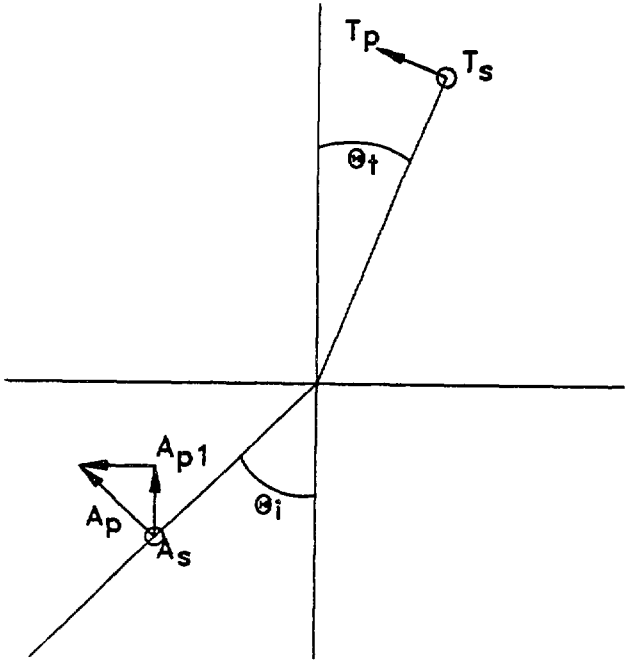

3) Refraction of a plane wave at the interface between two media. Plane of the paper is the plane of incidence. A_s, A_p, represent the amplitude of the incident electric field normal and parallel to the plane of incidence. T_s and T_p represent the amplitude of the transmitted electric field normal and parallel to the plane of incidence at the interface. A_{p1} is the component of the incident electric field normal to the interface, in the plane of incidence.

Experimental Results

The experimental arrangement for these measurements is similar to that shown in Fig. 1, except for the fact that the electrodes are rotated such that the angle of incidence is 45° (60° in some cases), another $\lambda/2$ plate is introduced in the beam and the cathode materials have optical quality surface finish. Figure 4 shows the reflectance and the corresponding electron yield measured for copper. Table 2 lists the ratios of $\frac{j_p}{j_s}$ and $\left(\frac{1-R_p}{1-R_s}\right)^N$ for various metals measured at 100 MW/cm^2. In all cases except gold, $\frac{j_p}{j_s}$ exceeds $\left(\frac{1-R_p}{1-R_s}\right)^N$ indicating an enhancement due to the optical field. Note: The measured $(1\text{-}R_p)$ and $(1\text{-}R_s)$ values relate to the intensity whereas Eqs. (4) and (5) are expressed in terms of the electric field associated with the laser that scales as the square root of the intensity.

Table II

Material	$\left[\frac{1-R_p}{1-R_s}\right]^N$ Measured at ~100 MW/cm^2	$\left(\frac{j_p}{j_s}\right)_{Vol+Surf}$
Ag Film	2.8	3.5
Au Film	10.3	9.4
Al Film	4.0	5.0
Cu–Diamond machined	2.8	15-25

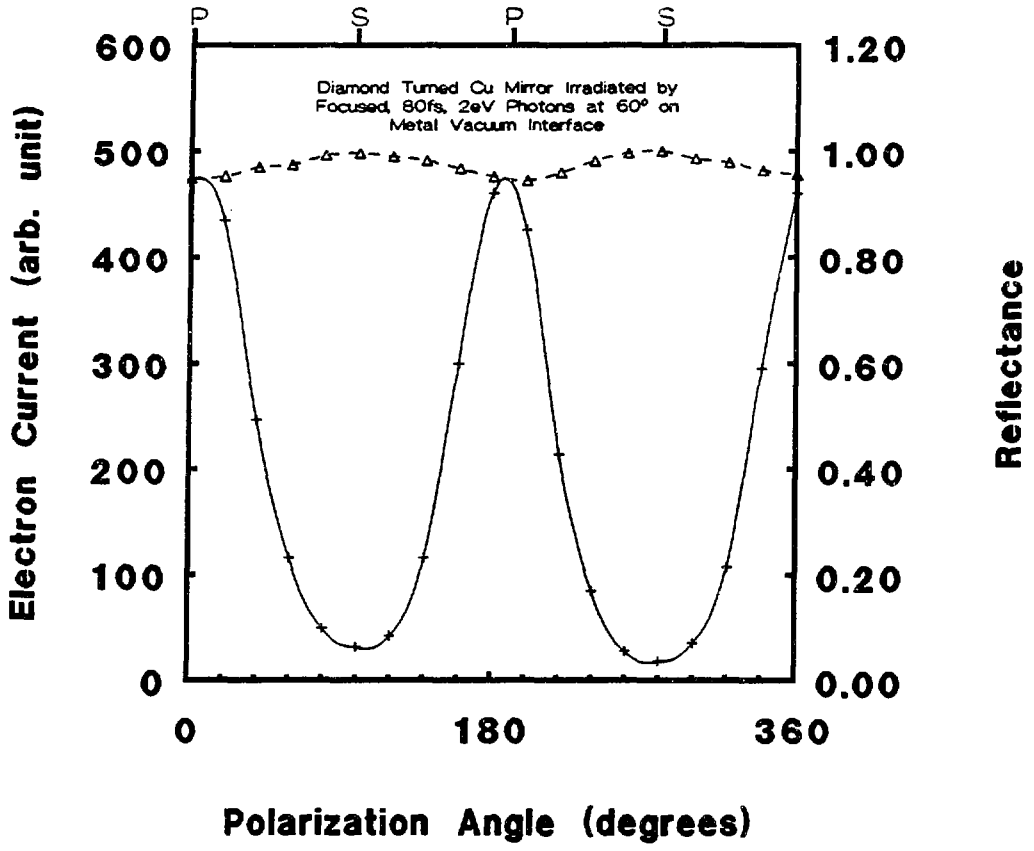

4) Polarization dependence of reflectance (Δ) and electron emission (+) for diamond-turned copper. The data points are connected for clarity.

ENHANCEMENT DUE TO SURFACE PLASMONS

Surface plasmons are collective oscillations of electron charge density that is confined to the surface of thin metal films. They are electromagnetic waves propagating along the metal dielectric interface, initiated by the discontinuity in $E_{\perp}$ of the optical field at the interface. Direct excitation of surface plasmons by the optical field is not possible since energy and

momentum cannot be conserved simultaneously during excitation. However, the component k_l of the momentum wave vector of the incident photon, parallel to the interface can be extended sufficiently by passing it through a prism at an angle larger than the critical angle of the prism so that the k_l of the photon matches that of the surface plasmon, i.e.,

$$k_l = \frac{\omega}{c}\sqrt{\frac{\epsilon_1\epsilon_2}{\epsilon_1+\epsilon_2}} \tag{6}$$

Where ω is the laser frequency, ϵ_1 and ϵ_2 are complex dielectric constants of the two media (medium 2 is assumed to be the plasmon active metal).

The active metals employed in these studies are Ag, Au, Cu and Al. Films with thickness appropriate for surface plasmon excitation are evaporated from a 99.99% purity wire under a vacuum of 10^{-6} Torr onto the hypotenuse side of a BK7 right angle glass prism. Electrical connections are made to the film subsequently and the metal-coated prism is transported to the experimental cell with minimum exposure to air, where it is pumped down to a pressure of 10^{-8}–10^{-9} Torr.

The experimental cell is very similar to the one described before except the cathode and the anode are replaced by the metal-coated prism and a Cu ring anode, respectively, with an electrode gap of 3 mm. The *p*-polarized laser beam is focused to a spot size of 5×10^{-5} cm^2 using a 15 cm focusing lens and irradiated at an angle of ~43° onto the metal film from

the glass side of the prism. The quasi DC current leaving the metal film is detected by an electrometer. Alternatively, lock-in technique has been used to avoid residual DC background.

Prior to the electron emission measurements, reflectance as a function of the angle of incidence in the vicinity of plasmon resonance angle (ATR spectrum) is measured using a collimated HeNe laser so that a theoretical fit to the experimental ATR spectrum using Fresnel reflection and transmission coefficients can be performed. Experimental data, theoretical calculations, the film thickness and metal dielectric constants used in the theoretical calculation are all displayed in Fig. 5.

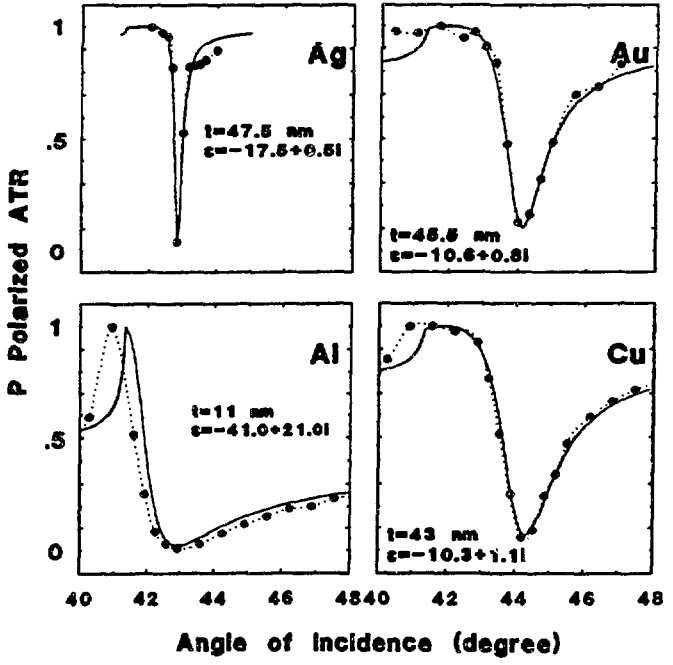

5) Experimentally measured ATR spectrum using unfocused HeNe laser (•) and theoretical fit to experimental data to determine the film thickness and dielectric constant (——).

The ATR spectrum and the electron emission are then simultaneously measured using the partially focused CPM laser beam at a vacuum pressure of $\sim 5\times10^{-9}$ Torr. Focusing is required to achieve the high laser power density needed for the nonlinear photoemission. However, efficient excitation of the plasmon mode depends critically on the purity of $k_{\parallel} = k\sin\Theta$. The small variation between the ATR spectra using collimated HeNe laser and the focused CPM laser is caused by the uncertainty in $k_{\parallel}$ associated with the bandwidth of the short laser pulse of the CPM and that of θ due to the focusing. The experimental ATR spectra, and electron emission are displayed in Fig. 6a. The corresponding theoretical ATR

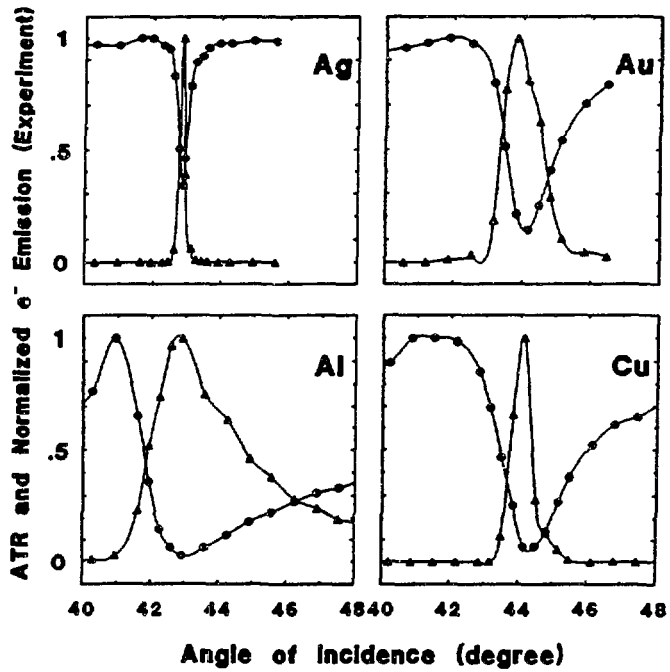

6a) Experimentally measured p-polarized reflectance (●) and multiphoton induced electron emission with surface plasmon excitation (Δ) as a function of the angle of incidence for various metals, using 625 nm, 90 fs laser pulses.

spectra and the electric field density at the metal vacuum interface $(E_1)^{2N}$ are displayed in Fig. 6b. The similarity between the electron emission data in Fig. 6a and $(E_1)^{2N}$ in Fig. 6b indicates that the electron emission is caused by the field component. It is interesting to note that the electron emission spectra are narrower than the ATR spectra by $\frac{1}{\sqrt{N}}$ as expected for an N photon process.

Figure 7 displays a logarithmic plot of input intensity vs. output current density for resonant (surface plasmon mediated) and non-resonant electron emission. The slope of the lines indicate N, the number of photons involved in the electron emission. The output current density for the two

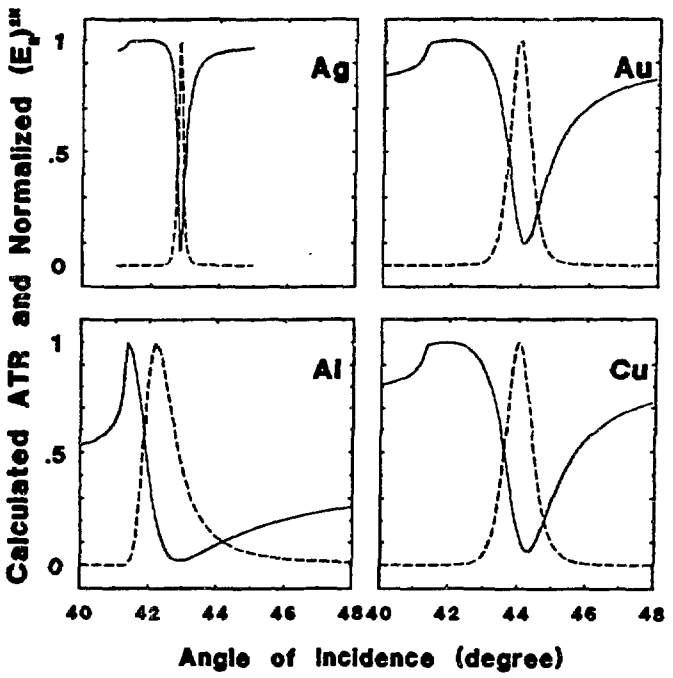

6b) Theoretical calculation of the reflectance of p-polarized light (——) and $(E_1)^{2N}$ (----) where E_1 is the parallel component of the electric field at the metal vacuum interface.

cases, at a given input intensity shows that the electron emission due to surface plasmons is up to 10^3 times larger than the nonresonant condition. This enhancement is commensurate with the increase in the field along the metal-vacuum interface of the surface plasmons when resonance conditions are met.

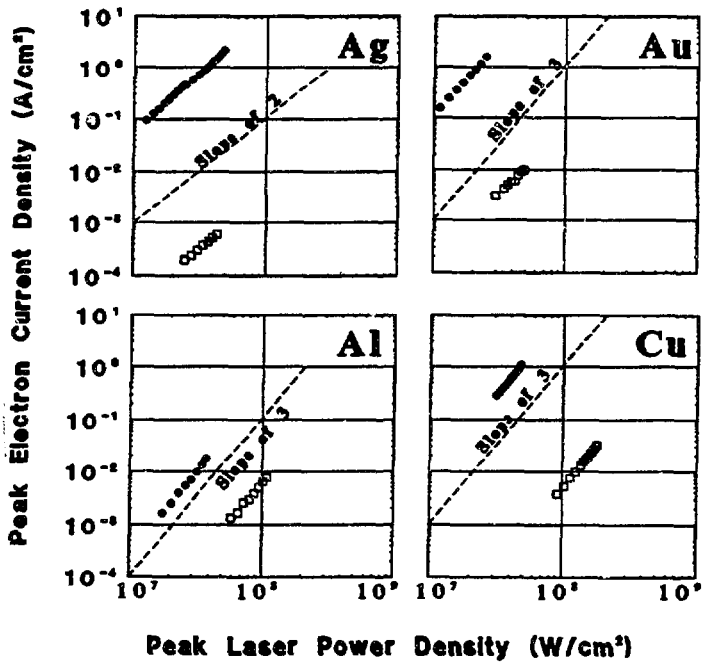

7) Electron current density vs the laser intensity for surface plasmon resonance (●) and nonresonant (□) excitation. The slope indicates the nonlinearity, N of the process. Comparison of current density obtained for the two cases at a constant input intensity indicates that the resonant excitation is 10^2–10^3 times more efficient than the nonresonant excitation.

PULSE DURATION MEASUREMENTS

The experimental arrangement of the previous section is slightly modified to incorporate two temporally identical and spatially overlapping CPM laser beams incidenting on the target. The time delay between the two beams are adjusted by including an optical delay line with a resolution of 0.1 μm in one of the beams. The output current as a function of the time delay between the two pulses and the autocorrelation trace of the laser are shown in Fig. 8. The width of the electron emission trace is almost the same as the laser autocorrelation trace. For a prompt N photon

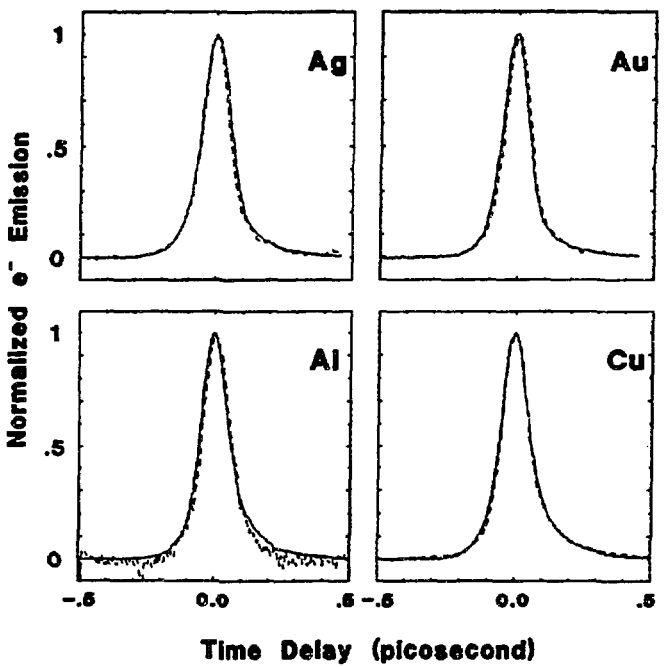

8) Electron emission as a function of the time delay between two identical spatially overlapping, 625 nm, 90 fs laser pulses (----) and the laser autocorrelator trace (——).

process, the width of the electron emission trace is expected to be $\frac{\tau}{\sqrt{N}}$ where τ is the pulse duration of the laser. The fact that the width of the electron emission curve is almost equal to that of the laser autocorrelation trace (a two photon process), instead of narrower by $\sqrt{\frac{2}{N}}$ is currently under investigation.

The absence of broadening at the wings indicate that at the intensities used, the temperature of the electrons is not high enough to make significant contribution to electron bunch due to thermionic emission.

CONCLUSION

In conclusion, the electron emission from a smooth surface can be increased by a factor of 2–15 by irradiating it with *p*-polarized light at oblique incidence. It can be enhanced substantially (up to 10^3) by exciting surface plasmons, which subsequently cause electron emission. An added advantage of this technique is the capability for back illumination of the film without the deleterious effects of photon absorption by the film. Extension of this method to obtain current densities exceeding 1 kA/cm^2 is subject to the limitation due to laser damage. Photoemission from both bulk and thin metal films indicate that at these laser intensities the electron emission is almost prompt and under emission limited conditions, electron pulse duration is similar to the laser pulse duration. Extrapolation of the

measured data to higher intensities indicate that current densities exceeding 10^5 A/cm^2 can be achieved at intensities well below the optical damage threshold of the bulk metal. However, effects of these high intensities on the emittance are yet to be explored.

REFERENCES

1. R. C. Fernow, "Proposal for a Study of Laser Acceleration of Electrons using Micrograting Structures at the ATF," page 65, BNL-43702, Brookhaven National Laboratory, Upton, NY, U.S.A. (1989).

2. R. B. Palmer, "Introduction" presented at the Workshop on "Prospects for a 1 Å Free Electron Laser," Sag Harbor, NY, April 22-27, 1990.

3. K. T. McDonald, "Proposal for an Experimental Study of Nonlinear Compton Scattering," page 183, BNL-43702, Brookhaven National Laboratory, Upton, NY, U.S.A. (1989)

4. R. W. Schoenlein, J. G. Fujimoto, G. L. Eesley and T. W. Capehart, "Femtosecond Studies of Image Potential Dynamics in Metals," Phys. Rev. Lett. 61, 2596 (1988).

5. J. Girardeau-Montaut and C. Girardeau-Montaut, "Space-charge-limited Current Density as a Function of Electron Flow Duration in an Emissive Diode," J. Appl. Phys. 65, 2889 (1989).

6. R. W. Schoenlein, W. Z. Lin, J. G. Fujimoto, and G. L. Eesley, "Femtosecond Studies of Nonequilibrium Electronic Processes in Metals," Phys. Rev. Lett, 58, 1680, (1987).

7. M. Born and E. Wolf, Principles of Optics (Pergamon Press, New York, 1980) page 40.